XLIII CILAMCE
21-25, November, 2022
FOZ DO IGUAÇU - PR - BRAZIL

Study of simplified elements for static and dynamic analysis of origami structures

Daniel Santos de Carvalho[1], Renan Costa Sales[1], Ney Augusto Dumont[1]

[1] *Department of Civil and Environmental Engineering, Pontifical Catholic University of Rio de Janeiro*
Rua Marquês de São Vicente, 225, - 22451-900 Rio de Janeiro – RJ, Brasil
danieng@hotmail.com, sales.rcosta@gmail.com, dumont@puc-rio.br,

Abstract. Research works involving structural origami have grown in recent years, especially applied to science and engineering problems. Early applications took advantage of the idea that a system can be folded compactly and subsequently deployed, and that self-assembly can be used to construct a three dimensional structure by starting from a thin sheet. The present work, as part of an M.Sc. thesis carried out by the first author, compares bar and hinge models with the simplest hybrid finite element models for plate and shell in order to represent origami structure panels. The bar and hinge model approach, as given in the literature, is based on folded patterns as pin-jointed truss frameworks: each vertex in the folded sheet is represented by a pin-joint, and every fold line by a bar element. The hybrid finite element formulation is based on the Hellinger-Reissner potential for an approximation of the stress field, thus satisfying the equilibrium equation of the elasticity problem in the domain and leading to a consistent structural model obtained at almost no additional cost when compared with the latter, too simplified, formulation. We assess the mechanical behavior of these structures and the folding energy measured in terms of the eigenvalues associated to the relevant eigenmodes of a cell for both the traditional bar and hinge scheme and the proposed equilibrium-based finite elements. The displacement response in time for a four-cell assemblage is also investigated for the implemented models.

Keywords: Hybrid finite element, bar and hinge model, plate and shells models.

1 Introduction

Research works involving structural origami have grown in interest in recent years, as especially applied to science and engineering problems. Pioneering applications took advantage of the idea that a system can be folded compactly and subsequently deployed, and that self-assembly can be used to construct a three dimensional structure by starting from a thin sheet [1]. It is worth mentioning that a quite recent, highly prized paper [2] by ASME, has managed to deal with bio-inspired origami metamaterials.

Several developments are reported to have used the finite element method [3, 4, 5] for the simulation of foldable structures in terms of refined mesh discretizations and demanding intensive computational effort. Expedite approaches rely on a bar and hinge model to represent an origami panel with few degrees of freedom, where the stiffness for the origami structure incorporates stiffness parameters for in-plane stretching and shearing, as well as panel bending and folding along prescribed lines [1, 6, 7]. The formulations of bar and hinge (and spring) models are based on information obtained from experimental works [8, 9] that evaluate the bending stiffness of elastic materials, as well as the bending line stiffness considering a length scale factor related to geometry and material fabrication properties [1, 10]. The basic implementation of the bar and hinge model is presented in [11].

On the other hand, we preferred to rely on the hybrid finite element method [12, 13] to represent the static and dynamic behavior of foldable structures, which also leads to the use of few degrees of freedom while trying to be as realistic as possible for the representation of linearly elastic plate and shell triangular elements under the hypothesis of small displacements. The implemented hybrid finite element method was born concomitantly with the hybrid boundary element method [14] based on works developed by Pian [15] and Reissner [16], which, when applicable, is more accurate than the displacement-based finite element method, as the domain interpolation functions are required to exactly already satisfy the problem's governing differential equations [17].

2 On the dynamic behavior of bar and hinge models according to the literature

The bar and hinge model N5B8 proposed by Filipov et al [1] has 5 nodes and 8 bars, as on the right of Fig. 1, in order for the origami structure to incorporate stiffness parameters for in-plane stretching and shearing, as well as panel bending and folding along prescribed lines, according to the stiffness properties

$$k_B = \mathrm{C}_B \frac{Et^3}{12\;\; 1-v^2}\left(\frac{D_s}{t}\right)^{\frac{1}{3}}, \quad k_l = \frac{L_F}{L^*}\frac{Et^3}{12\;\; 1-v^2} \tag{1}$$

We recognize in these equations the thin plate's stiffness given in terms of the elasticity modulus E, the thickness t and the Poisson's ratio ν. The equation on the left, for bending stiffness, also features the smallest element diagonal D_s and a constant C_B obtained empirically to best fit the bar and hinge model to the cases of small and large displacements. Because two rotational hinges are used on each diagonal of the panel, half of the corresponding stiffness, $k_B / 2$, is alternatively attached to each rotational constraint [1]. However, this approach is not cited in more recent works by the authors [3, 6, 11, 18]. The introduced *folding stiffness* k_l is expressed in terms of the edge's length of folding L_F and a length scale L^* obtained empirically in terms of the material's mechanical properties [10].

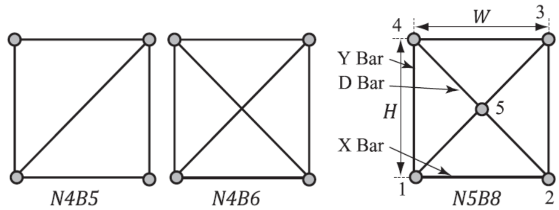

Figure 1. Evolution of the bar and hinge models with N nodes and B bars [1].

The dynamic behavior of the bar and hinge coupled system was simulated by Filipov et al [1] with the plate's total mass distributed either equally among the nodes, with a lumped matrix called "bar model 1", or consistently, as a "bar model 2", according to Carvalho [19]. This may actually lead to very cumbersome expressions – albeit consistent in the proposed framework. Moreover, the authors propose to express the folding and bending stiffness degrees of freedom in terms of the relative out-of-plane displacements of the cell, for the bars considered always straight while liable to axial deformation, as illustrated in Fig. 2b, thus significantly reducing the number of a cell's degrees of freedom, which end up to be just three per indicated node. A reasonable – although no longer up-to-date – summary of the accomplishments by Paulino, Filipov and co-workers is given by Carvalho [19].

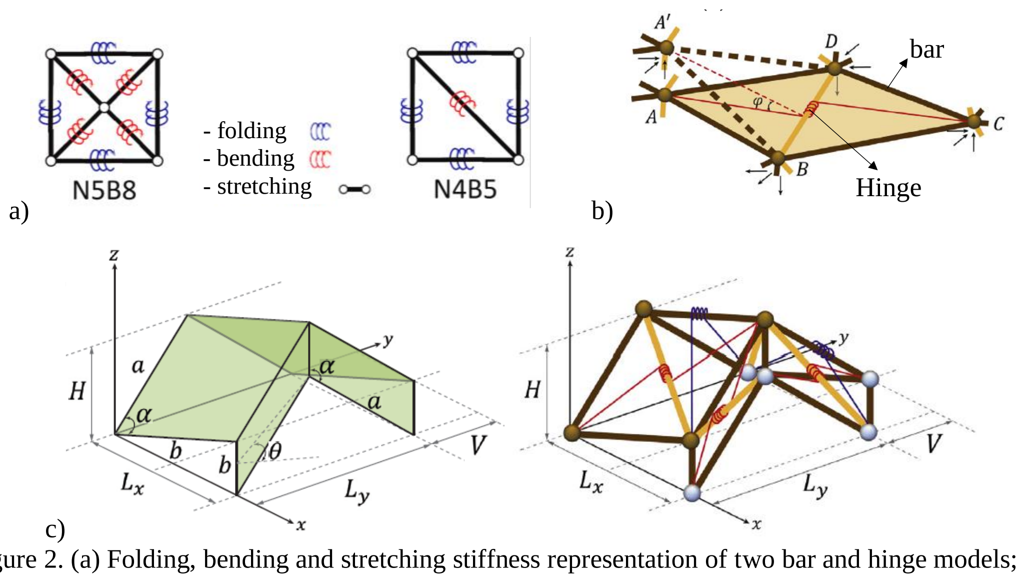

Figure 2. (a) Folding, bending and stretching stiffness representation of two bar and hinge models; (b) deformed configuration of model N4B5; (c) Miura-ori cell (Liu and Paulino [11], Pratapa et al [18]).

3 Implemented hybrid/displacement finite membrane and plate elements

Owing to space restrictions we shall not present a review of the hybrid finite element method [17, 20, 21]. Sales [13] has managed to make some key developments of general membrane and plate hybrid finite elements for the simulation of the dynamic behavior of structures. However, we are only concerned with investigating some models that may rival in simplicity with the bar and hinge systems featured above while reproducing more consistently the static and dynamic behavior of complex origami structures that are just made of foldable panels. So, we decided to explore and combine the simplest membrane – the constant strain – element and the simplest plate – the constant curvature – element [13, 19]. The former element is just called CST and the latter one has been firstly proposed by Morley [22]. It is noteworthy that the stiffness and mass matrices of these two elements can in principle be obtained indifferently in terms of either the displacement or the hybrid finite element method. However, Sales [23] shows that evaluations in the frame of a generalized modal analysis, for which a frequency power series of the problem's effective stiffness matrix is required, can only be carried out in the frame of the hybrid formulation proposed by Dumont and Oliveira [24].

3.1 Basics on our proposed implementations

The simplest hybrid finite elements implemented [13] and tested by Carvalho [19] can be summarized as
HT3 – Three-node triangular (CST) element with two in-plane degrees of freedom per node (Fig. 3a).
HKPT6 – Three-node triangular thin-plate (Morley) element with one transversal degree of freedom (*dof*) per node and one rotational *dof* along each side (Fig. 3b).
HS3 – Hybrid shell element obtained as the combination of elements HT3 and HKPT6 (Fig. 3c).

The "K" in plate element HKPT6 stands for Kirchhoff, as we are considering thin plates. Sales [25] presents the formulation for moderately thick elements while consistently including the inertia effect.

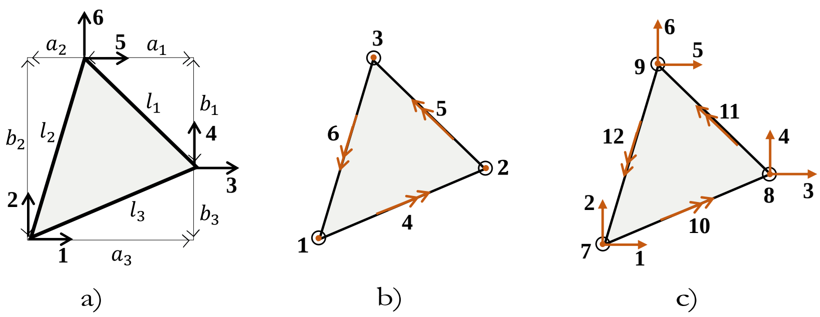

Figure 3. a) Membrane HT3, b) plate HKPT6, and c) shell HS3 elements.

3.2 Stiffness matrix including the folding effect between two adjacent panels

As proposed for the plate element HKPT6 of Fig. 3b, the rotational degrees of freedom 4, 5 and 6 are used to provide rotational continuity between the edges of two adjacent elements. However, if the panel is folded along one edge, the rotational continuity between panels is no longer preserved and we should consider as the best – while simplified – approach that such edge would work as a hinge with the attached elastic stiffness k_l of Eq. (1) already proposed by Filipov et al [1].

The folding stiffness introduced above was incorporated by Carvalho [19] into the plate element HKPT6 of Fig. 2b, as shown in Fig. 4 for the edge related to the rotational *dof* 6, by considering that this *dof* is actually internal to the element and the rotational spring stiffness k_l of Eq. (1) is then attached to it so that the system becomes kinematically determined. In one further step, we condense the internal *dof* 6 statically and obtain the condensed plate stiffness matrix

$$\mathbf{K}_{\mathrm{p}} = \begin{bmatrix} \mathbf{K}_{ee} - \dfrac{1}{K_{ii} + k_l}\mathbf{K}_{ei}\mathbf{K}_{ie} & \dfrac{k_l}{K_{ii} + k_l}\mathbf{K}_{ei} \\ \dfrac{k_l}{K_{ii} + k_l}\mathbf{K}_{ie} & \dfrac{K_{ii}k_l}{K_{ii} + k_l} \end{bmatrix} \tag{2}$$

where $\mathbf{K}_{ee}$ is the matrix of order 5 for the "*e*" external *dof*s 1-5 and the index '*i*' corresponds to the original *dof* number 6 as if considering rotational continuity. For this static condensation to take place, as proposed, we are assuming that the attached spring, *dof* 7, has stiffness k_l but is otherwise massless.

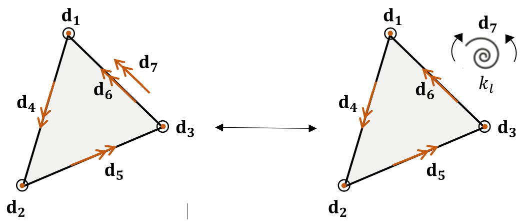

Figure 4. Plate element HKPT6 of Fig. 3b for attached rotational spring with stiffness k_l.

3.3 Mass matrix of the hybrid elements

The inertia effect is taken into account in terms of a mass matrix only, although a more refined, generalized, approach has also been implemented and tested [23]. The consistent mass matrix of the membrane element HT3 is the same one of the classical literature [19] and shall not be repeated here. For the plate element HKPT6, we use as displacement shape functions

$$\begin{bmatrix} N_1 \\ N_2 \\ N_3 \\ N_4 \\ N_5 \\ N_6 \end{bmatrix} = \begin{bmatrix} 1 & 0 & 0 & \frac{1}{2}\,1+e_2 & \frac{1}{2}\,2+e_2-e_3 & \frac{1}{2}\,1-e_3 \\ 0 & 1 & 0 & \frac{1}{2}\,1-e_1 & \frac{1}{2}\,1+e_3 & \frac{1}{2}\,2+e_3-e_1 \\ 0 & 0 & 1 & \frac{1}{2}\,2+e_1-e_2 & \frac{1}{2}\,1-e_2 & \frac{1}{2}\,1+e_1 \\ 0 & 0 & 0 & 0 & 2A/\ell_3 & 2A/\ell_3 \\ 0 & 0 & 0 & 2A/\ell_1 & 0 & 2A/\ell_1 \\ 0 & 0 & 0 & 2A/\ell_2 & 2A/\ell_2 & 0 \end{bmatrix} \begin{bmatrix} \xi_1^2 \\ \xi_2^2 \\ \xi_3^2 \\ \xi_1\xi_2 \\ \xi_2\xi_3 \\ \xi_3\xi_1 \end{bmatrix} \tag{3}$$

as proposed by Abdalla & Hassan [26] (with some misprints that have been fixed by Sales [23]). In this equation, ξ_i are the triangle natural coordinates, A is the area, ℓ_i are the edge lengths and

$$e_i = \frac{\ell_k^2 - \ell_j^2}{\ell_i^2} \tag{4}$$

are the triangle *excentricities*.

The procedures for the complete evaluation of the membrane's and plate's mass matrices are described by Carvalho [19] on the basis of the more general developments by Sales [23] and shall not be reproduced here.

4 Numerical comparisons with Filipov et al's approach

We carry out next some comparisons of the bar and hinge model developed by Filipov et al [1] and our proposed hybrid element model, as part of the implementations proposed in Carvalho's M.Sc. thesis [19]. The most important features are best assessed in terms of the elastic energy developed for some plane and spatial configurations and measured in terms of some key eigenvalues. We also display some dynamic results for a four-cell assemblage, where a cell is itself the assemblage of four triangle elements. It is worth remarking that, although not implemented by Carvalho, we might carry out the dynamic condensation (more consistently than a static condensation – *Guyan reduction*) of the 7 internal *dof*s of a cell made up of four triangle elements, thus reducing the initial number of 23 *dof*s to 16 *dof*s, just one more than the 15 *dof*s of the bar and hinge model – while preserving the internal stiffness and inertia properties of the hybrid finite elements.

4.1 Geometric analysis for a cell

Figure 5 displays on the left the eigenvalue λ_1 corresponding to the static, torsion eigenmode of square cells of varying length starting from $L = 1\,m$ (elasticity modulus $E = 1\,GPa$, Poisson's ratio $\nu = 1/3$ and thickness $t = 0.01\,m$). The expedite bar and hinge model featured in Section 2 is assessed for either half the stiffness for each rotational constraint, *bar* $(k_B/2)$, or its integral value, *bar* (k_B). The solid (red) line in this figure shows the results obtained with our approach, which is entirely consistent and does not resort to the empirical values of Eq. (1). On the right of Fig. 5 are the torsional eigenvalue results for a cell of unity edge length but with the indicated angle α varying from 15^0 to 45^0.

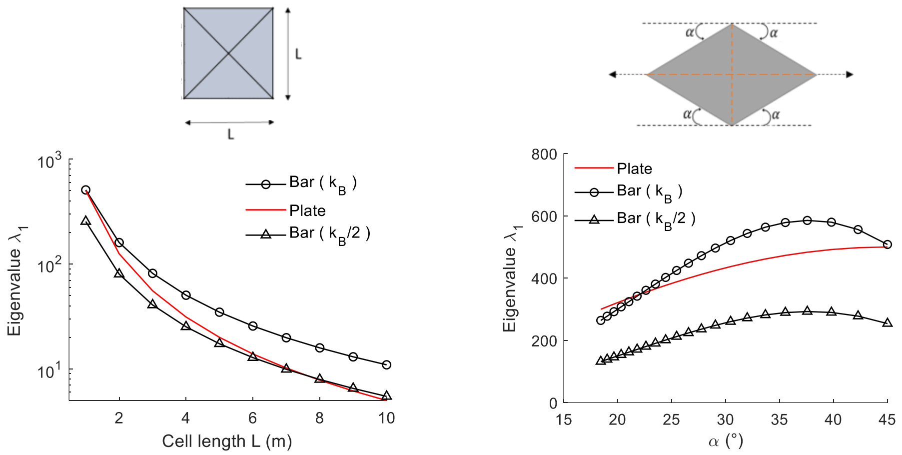

Figure 5. Torsional eigenvalue for square cells with varying length, and for distorted cells of unit edge length.

Figure 6 shows on the left the configuration for a cell folded [1]. The eigenvalue results for the eigenmode representing relative rotation of the cells are shown on the right for relative folded positions varying from 0^0 to 15^0 and plate thicknesses 8, 10 and 12 mm. The bar and hinge model results are for *bar* (k_B).

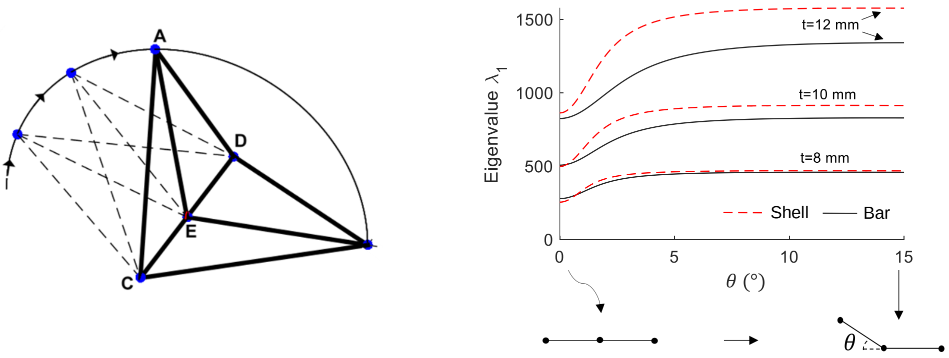

Figure 6. Folding a cell and graph with spatial configuration for angle $\theta = 0^0$ to 15^0 showing the eigenvalue results for plate thicknesses 8, 10 and 12 mm.

4.2 Displacement time analysis for four cells

Owing to space restrictions, we jump for the analysis of a transient problem (several other interesting comparisons are given by Carvalho [19]). Figure 7 shows on the top a four-cell panel comprising 16 triangles. The initial configuration has the indicated out-of-plane inclination $\theta = 60^0$ of the panels. Nodes 6 and 7 are fully constrained. Constant (step-function) unit forces F are applied in the *x* direction of nodes 1, 2, 12, 13 and, since the structure is symmetric, *x*-displacements at nodes 1 (as the same for node 2) and 3 (as the same for node 4) are evaluated in the direction *x*, while *z*-displacements are evaluated at node 3 (as the same for node 4). The subsequent graphs show the *x* and *y* displacements along time obtained by Carvalho [19] in the frame of a modal analysis for all implemented simulations. The second mass distribution for the expedite *bar model 1*, according to Section 2, shows a bad time response to the applied load excitation. On the other hand, the *bar model 2* leads to relatively good results when compared to our consistent developments.

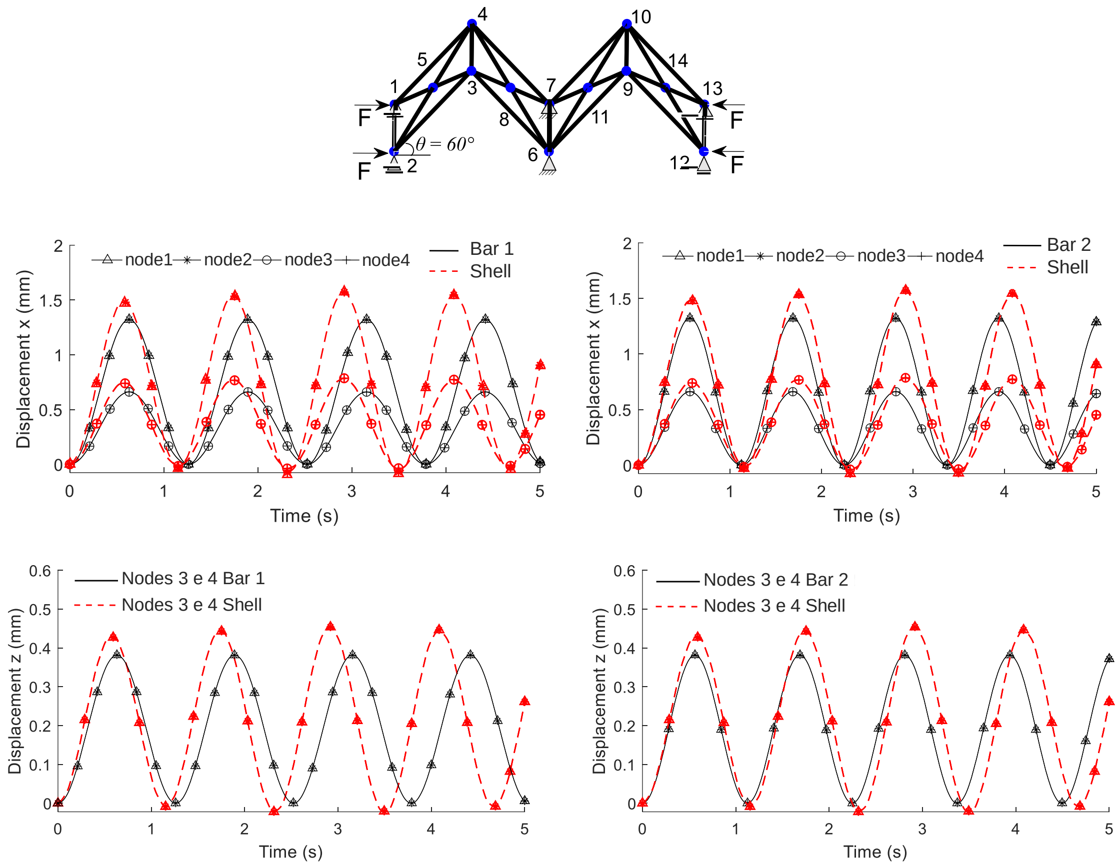

Figure 7. Four-cell structure on the top, and horizontal and vertical displacement comparisons of our proposed shell model with the expedite bar and hinge approaches of Section 2.

5 Conclusions

The implemented hybrid finite plate and shell elements have shown to be a robust, reliable solution to simulate an origami structure and as economical as the proposed bar and hinge models of the literature. Moreover, the hybrid elements do not need any artificialities to resort to as they are directly derived from a consistent energy approach. Since we are dealing with very simple structures, no dynamic condensation of a cell´s internal *dof*s has been carried out in the finite element simulations of the numerical illustrations. With the consistent, dynamic condensation, the initial numbers of 23, 39 and 71 *dof*s for one, two and four cells would be reduced to 16, 25 and 43, which are just one *dof* more as compared with the respective bar and hinge structures (15, 24 and 42).

The linear dynamic analysis showed that the bar and hinge models perform just satisfactorily for the *bar model 2*. We should expect large deviations from our consistent model if large panels are considered, although the faulty mass distribution of a single cell might get smeared. This remains to be investigated, as we are proposing that our model should in fact replace the expedite bar and hinge system in any computer simulations of origami structures.

We are planning as a future work the implementation of our model for panels undergoing large displacements in the frame of a co-rotational approach – a technique that seems well consolidated in the technical literature since some pioneering works as the one by Shabana and Wehage [27].

Authorship statement. The authors hereby confirm that they are the sole liable persons responsible for the authorship of this work, and that all material that has been herein included as part of the present paper is either the property (and authorship) of the authors or has the permission of the owners to be included here.

References

[1] E. T. Filipov, K. Liu, T. Tachi, M. Schenk and G. H. Paulino. Bar and hinge models for scalable analysis of origami. *International Journal of Solids and Structures*, vol. 124, pp. 26-45, 2017.
[2] K. Liu, T. Tachi and G. H. Paulino. Bio-inspired origami metamaterials with metastable phases through mechanical phase transitions. *Journal of Applied Mechanics*, vol. 88, n. 9, p. 091002 (10 pp), 2021.
[3] M. Schenk and S. D. Guest. Origami folding: A structural engineering approach. In P. Wang-Iverson. R. Lang. M. Yim, ed, *Origami 5: Fifth International Meeting of Origami Science, Mathematics, and Education*, pp. 293-305, 2011.
[4] C. Lv, D. Krishnaraju, G. Konjevod, H. Yu and H. Jiang. Origami based mechanical metamaterials. *Scientific Reports*, vol. 4, pp. 5979-5981, 2014.
[5] J. M. Gattas and Z. You. The behaviour of curved-crease foldcores under low-velocity impact loads. *International Journal of Solids and Structures*, vol. 53, n. 15, pp. 80-91, 2015.
[6] E. T. Filipov, T. Tachi and G. H. Paulino. Toward optimization of stiffness and flexibility of rigid, flat-foldable origami structures. In T. Kawasaki. R. Uehara. T. Tachi. J. Maekawa, ed, *The 6th International Meeting on Origami in Science, Mathematics and Education*, pp. 121, 2015.
[7] M. Schenk. *Folded shell structures*. PhD thesis, University of Cambridge, 2012.
[8] A. E. Lobkovsky, S. Gentges, H. Li, D. Morse and T. A. Witten. Scaling properties of stretching ridges in a crumpled elastic sheet. *Science*, vol. 270, n. 5241, pp. 1482-1485, 1995.
[9] C. Pradier, J. Cavoret, D. Dureisseix, J. C. Mistral and F. Ville. An experimental study and model determination of the mechanical stiffness of paper folds. *Journal of Mechanical Design*, vol. 138, n. 4, pp. 041401, 2016.
[10] F. Lechenault, B. Thiria and M. Adda-Bedia. Mechanical response of a creased sheet. *Physical Review Letters*, vol. 112, n. 24, pp. 244301, 2014.
[11] K. Liu and G. H. Paulino. Nonlinear mechanics of non-rigid origami: an efficient computational approach. *Proceedings of the Royal Society A*, vol. 473, pp. 1-28, 2017.
[12] N. A. Dumont and P. G. C. Prazeres. Hybrid dynamic finite element families for the general analysis of time-dependent problems. In *ICSSD 2005 - Third International Conference on Structural Stability and Dynamics*, pp.10 on CD, Florida (USA), 19-22 Jun 2005.
[13] R. C. Sales. *Implementação de elementos finitos híbridos planos para a análise de placas e cascas finas ou moderadamente espessas*. Master's thesis, Pontifical Catholic University of Rio de Janeiro. (In Portuguese), 2018.
[14] N. A. Dumont. The hybrid boundary element method: an alliance between mechanical consistency and simplicity. *Applied Mechanics Reviews*, vol. 42, n. 11, Part 2, pp. S54-S63, 1989
[15] T. H. H. Pian and P. Tong. Basis of finite element methods for solid continua. *International Journal for Numerical Methods in Engineering*, vol. 1, pp. 3-28, 1969.
[16] E. Reissner. On a variational theorem in elasticity. *Journal of Mathematics and Physics*, vol. 29, pp. 90-95, 1950.
[17] P. G. C. Prazeres. *Desenvolvimento de elementos finitos híbridos para a análise de problemas dinâmicos usando superposição modal avançada*. Master's thesis, Pontifical Catholic University of Rio de Janeiro. (In Portuguese), 2005.
[18] P. P. Pratapa, P. Suryanarayana and G. H. Paulino. Bloch wave framework for structures with nonlocal interactions: Application to the design of origami acoustic metamaterials. *Journal of the Mechanics and Physics of Solids*, vol. 118, pp. 115-132, 2018
[19] D. S. de Carvalho. *Estudo de elementos simplificados para a análise estática e dinâmica de estruturas origami*. Master's thesis, Pontifical Catholic University of Rio de Janeiro. (In Portuguese), 2020.
[20] N. A. Dumont and C. A. Aguilar. Linear algebra issues in a family of advanced hybrid finite elements. In R. D. V. Kutis. J. Murín, ed, *Computational Modelling and Advanced Simulations*, Computational Methods in Applied Science, chapter 14, pp. 255-275, Springer, Verlag, 2011.
[21] N. A. Dumont and P. G. C. Prazeres. A family of advanced hybrid finite elements for the general analysis of time-dependent problems and non-homogeneous materials. *Proc. XXV CILAMCE – XXV Iberian Latin-American Congress on Computational Methods in Engineering*, pp. 15 on CD, 2004.
[22] L. S. D. MORLEY. The constant-moment plate bending element. *The Journal of Strain Analysis for Engineering Design*, vol. 6, pp. 20–24, 1971.
[23] R. C. Sales. *Implementation of frequency-dependent hybrid finite elements for the analysis of thin or moderately thick plates and shells*. PhD thesis, Pontifical Catholic University of Rio de Janeiro. (In progress), 2022.
[24] N. A. Dumont and R. Oliveira. From frequency-dependent mass and stiffness matrices to the dynamic response of elastic systems. *International Journal of Solids and Structures*, vol. 38, pp. 1813-1830, 2001.
[25] N. A. Dumont and R.C. Sales. Consistency assessment of plate bending theories for the implementation of efficient hybrid finite elements in linear statics and dynamics. *Proc. of the XLII Ibero-Latin-American Congress on Computational Methods in Engineering and III Pan-American Congress on Computational Mechanics*, 2021.
[26] H. Abdalla and K. Hassan. Shape effect on Morley's element. *Communications in Applied Numerical Methods*, vol. 1, pp. 255-259, 1985.
[27] A. A. Shabana and R. A Wehage. A coordinate reduction technique for dynamic analysis of spatial substructures with large angular rotations, *Journal of Structural Mechanics*, vol. 11, pp. 401–431, 1983.